RSC Advances

This is an *Accepted Manuscript*, which has been through the Royal Society of Chemistry peer review process and has been accepted for publication.

Accepted Manuscripts are published online shortly after acceptance, before technical editing, formatting and proof reading. Using this free service, authors can make their results available to the community, in citable form, before we publish the edited article. This *Accepted Manuscript* will be replaced by the edited, formatted and paginated article as soon as this is available.

You can find more information about *Accepted Manuscripts* in the Information for Authors.

Please note that technical editing may introduce minor changes to the text and/or graphics, which may alter content. The journal's standard Terms & Conditions and the Ethical guidelines still apply. In no event shall the Royal Society of Chemistry be held responsible for any errors or omissions in this *Accepted Manuscript* or any consequences arising from the use of any information it contains.

ROYAL SOCIETY OF CHEMISTRY

www.rsc.org/advances

Manuscript submitted for publication in ***RSC Advances***

Aminosilane decorated carbon template-induced in situ encapsulation of multiple-Ag-cores inside mesoporous hollow silica

Fu Yang, Saifu Long, Shijian Zhou, Xiaoming Li, Xianfeng Liu, Shuying Gao, Yan Kong*

State Key Laboratory of Materials-Oriented Chemical Engineering, College of Chemistry and chemical engineering, Nanjing Tech University, Nanjing 210009, China

RSC Advances Accepted Manuscript

State Key Laboratory of Materials-Oriented Chemical Engineering

Nanjing Tech University, Nanjing 210009

Corresponding Author. Email: *kongy36@njtech.edu.cn*; Tel & Fax: 86-025-83587860

Abstract: Dispersed and stable catalytic active phase and protective reaction environment are acknowledged as ideal metal catalyst characteristics. In this paper, a Cores@Shell structure of microreactor with well-dispersed active phase of multiple free-Ag-cores, hollow cavity and protective mesoporous shell was prepared by a simple and novel constructed approach. The organic ligand of aminosilane (APTES) was directly incorporated on the carbon nanosphere to anchor Ag ions as metallotemplate, which avoids conventional methods of tedious steps, and then the sacrificed metallotemplate was employed for directly fabricating the special hollow mesoporous silica microreactor. As a result, multiple free active Ag-cores were in situ produced and encapsulated in cavity of hollow mesoporous silica during the thermal process. The important evidences of configuration including big hollow cavity containing active multiple-Ag nanoparticles and mesoporous SiO_2-shell can be demonstrated with efficient techniques including XRD, FT-IR, XPS, BET, SEM and TEM. Just as expected, the catalyst as a functional microreactor exhibited a high catalytic activity for the liquid-reduction of 4-nitrophenol, and the increasing dosage of used catalyst contributes to the enhancing of catalytic activity. The methodology demonstrated here provides a new insight for the fabrication of versatile functional nanosmaterials with kinds of noble or transition metals inside hollow shell.

Keywords: Aminosilane, Multiple-Ag-cores, Carbon nanosphere, Mesoporous silica, Microreactor.

RSC Advances Accepted Manuscript

1. Introduction

The design and fabrication of nanospherical materials with hollow interiors exhibited huge potential uses as low-density capsules for controlled release of drugs,[1, 2] development of artificial cells,[3] protection of enzymes,[4] proteins[5] and DNA,[6] especially for catalysis.[7-9] Wherein, hollow mesoporous silica sphere is regarded as an ideal nanoreactor due to its narrow mesochannels in the shell and large hollow intra-cavity, which have attracted considerable attention in the nanomaterial fields.[10-13] This special morphology of carrier can accommodate the catalytic active phase and reactants and allow the chemicals to be transported in and out of the reactor via mesochannels, which could efficiently improve the conversion of reactant and selectivity of product.

Generally, contacting, collision between reactant and catalytic active sites and diffusion of chemicals in microscale reactors are regarded as key impacts in determining conversion and selectivity of chemicals. Therefore, a functional nanoreactor, possessing dispersed active phase and large diffused region, would be expected to obtain high catalytic activity. Fully functional nanoreactors can be realized using porous hollow spheres attaching highly-efficient catalytic active phase. So far, many attempts have been employed to encapsulate some special chiral metal complexes or noble metals into mesoporous silica nanocages just like Ship-in-bottle.[11, 14-17] The resulting catalytic system shows remarkable activity and recyclability for asymmetric synthesis and other kinds of reactions. Noble metal nanoparticles (NPs), especially for silver nanoparticles, have been widely studied due to their unique catalytic activities in hydrogenation reduction and compelling cost-efficience in practical applied process as compared to other counterparts.[18, 19]

RSC Advances Accepted Manuscript

The study found that restricting noble metal NPs in isolated nanocavity can effectively avert some defects such as noble metals' aggregation, sintering and rapid decay of catalytic activity.[15] In order to obtain the isolated active phase, single core@porous-shell architectures have been proposed and well applied in heterogeneous catalysis.[12, 20-22] The result revealed that the freely movable core contributes to high catalytic activity, and its hollow cavity and the protective shells provide a homogenous environment for the heterogeneous catalysis. However, a more attractive structure possessing multiple active cores, hollow cavity and porous shell is obviously superior to the previous one due to the high contribution of multiple free active cores for enhancing the collision frequency with reactant molecules.[23] Some strategies have been developed to combine these advantages for obtaining the expected functional catalyst.[23-25] Wherein, the synthesis of these special nanoreactors mainly involves the modification of sacrificial template through depositing noble metal particle on their surface.[15, 26, 27] However, there is still plenty of room for further improvement using new synthetic technology to simplify the conventional methods of tedious steps. As we know, surface of carbon sphere from the hydrothermal method is enriched with hydroxide radicals, and these active groups on the carbon sphere can be well utilized by tethering other special species to obtain functional carbon sphere. However, so far, there is still no any report involving organic modification of carbon sphere and its further application to anchor metal ions species. Inspired by these thoughts, a new tactic involving organic modification of carbon sphere and its further utilization as functional hard template to prepare hollow microreactor is desirable to develop.

In this study, we reported an approach, for the first time, to in situ encapsulate multiple

RSC Advances Accepted Manuscript

active Ag-core nanoparticles inside hollow mesoporous silica sphere for further improving efficiency of core@shell. The carbon sphere was first decorated with metal-capturing agent of aminosilane (APTES) to anchor Ag ions. Then, the Ag-aminosilane functional carbon sphere acted as sacrificed template for preparing the special hollow mesoporous microreactor. In this structure, the free Ag nanoparticles within the inner cage of hollow mesoporous silica sphere as catalytic active sites were fully accessible for reactants. The specific synthesized route could refer to the Scheme 1. The involving samples were characterized using different techniques for demonstrating the morphology and structure, status of Ag NPs and the proposed synthesized method. Finally, the obtained hollow Ag@meso-SiO_2 was applied for the catalytic reduction of 4-nitrophenol to evaluate its catalytic performance and different accounts of Ag@meso-SiO_2 were utilized to investigate the effects on reaction.

2. Experimental

2.1. Chemicals

Glucose, tetraethylorthosilicate (TEOS), ammonia solution (25 wt%), silver nitrate ($AgNO_3$), L-arginine and cetyltrimethylammonium chloride (CTAC) were purchased from Sinopharm Chemical Reagent Co., Ltd. 3-aminopropyltriethoxysilane (APTES) was purchased from the Tokyo TCI (Shanghai) Development Co., Ltd. 4-nitrophenol and sodium borohydride were purchased from Aladdin. Commercial Ag nanoparticles were purchased from Zhuhai Najin Technology (Guangdong) Co., Ltd. All the chemicals were used as received without further purification.

RSC Advances Accepted Manuscript

2.2. Synthesis of multiple-Ag-cores hollow microreactor

2.2.1. Synthesis of carbon nanospheres (CNs)

The synthesis of carbon sphere is based on the reference.[15] Typically, Glucose (9 g) was dissolved in 60 mL water to form a clear solution and then transferred into an 80 mL Teflon-sealed autoclave. The autoclave was maintained at 190 ºC for 5 h. The products were separated by centrifugation, followed by washing three times using water and ethanol respectively and finally oven-dried at 80 ºC for further use.

2.2.2. Silanization of CNs and anchoring of Ag ions

In this typical process, 100 mg carbon nanospheres were dispersed in 100 mL deionized water with ultrasonic for 45 min as part A. 0.2 ml APTES was dissolved in 6 mL deionized water as part B. Parts A and B were mixed together and reflux condensed in 75 °C water bath for 6 h. Then the suspension was centrifuged and washed with distilled water five times. The resulting product was designated as NH_2-CNs. Then, the NH_2-CNs composite obtained from last step was redispersed in the aqueous solution containing certain amount of $AgNO_3$ and stirred for 4 h. Finally, the suspension was centrifuged and washed again and the final product was labelled as Ag/NH_2-CNs.

2.2.3. Preparation of Ag@meso-SiO_2

Subsequently, the Ag/NH_2-CNs composite were redispersed in 40 mL H_2O, 30 mL ethanol, 0.132 g of CTAC and 568 μL of $NH_3 \cdot H_2O$ with ultrasonic for 20 min. Then 150 μL of

RSC Advances Accepted Manuscript

TEOS was added, and the mixture was vigorously stirred for 6 h. The precipitate was harvested after centrifuged and washed with distilled water and with ethanol for three times, then dried at 60 ºC for 6 h. Then the product was calcined at 550 ºC for 6 h then in air atmosphere for 6 h to remove carbon sphere, CTAC template and other organic species. The finally obtained Ag@meso-SiO_2 product was further employed as catalyst for liquid-phase reduction of 4-nitrophenol reaction.

2.2.4. Synthesis of comparative catalysts

Ag-supported SBA-15 materials was synthesized according to the reported literature,[28] typically, 1 g of P123, 30 g of deionized water and 3 g of nitric acid were mixed and stirred for 1 h at 35 °C until a homogenous solution formed under acidic conditions. Meanwhile, certain amount of silver nitrate was added to the solution and stirred for 1 h. Then, 2.13 g of TEOS was added into the solution and stirred for 20 h at 35 °C in the dark. The derived solution was aged at 100 °C for 48 h. The product was filtered off, rinsed with deionized water for several times. The resulting powders were calcined at about 550 °C for 5 h in air to obtain Ag/SBA-15.

The synthesis of single core Ag@SiO_2 material is based on the reported literature,[29] 7.5 mL of aqueous solution of glucose (30 mg/mL) was added into a mixture of water and CTAB (50 mg in 40 mL) previously heated at 80 °C for 30 min followed by dropwise addition of an aqueous solution of silver nitrate and arginine (54 mg and 56 mg respectively in 1.5 mL of water). After 3 min, an additional amount of CTAB (50 mg) was added to the solution, followed by dropwise addition of TEOS (1060 μL). The resulting brown solution was stirred at 500 rpm at 80 °C for 3 h. Finally, the resulting sample was collected, washed and

RSC Advances Accepted Manuscript

calcined at 550 °C for 5 h in air to obtain single core Ag@SiO_2.

2.3. Characterizations

X-ray diffraction patterns were recorded using a Smartlab TM 9 KW powder diffractometer with a monochromatic Cu K_α source radiation (λ= 1.5406 A°).

Fourier Transform Infrared (FT-IR) spectra of the samples were obtained in the range of 400-4000 cm^{-1} with powders dispersed on KBr on Bruker VECTOR22 resolution.

The X-ray photoelectron spectra (XPS) were performed on a PHI 5000 Versa Probe X-ray photoelectron spectrometer equipped with Al K_α radiation (1486.6 eV). The C1s peak at 284.6 eV was used as the reference for binding energies.

The N_2 (77.4 K) adsorption-desorption measurements were carried out with Micromeritics ASAP-2000 instrument in a relative pressure range P/P_0 from 0.01 to 0.99, and before the measurements, the calcined samples were outgassed in vacuum at 150 °C for 5 h. The specific surface area and pore size distribution were calculated by the Brunauer-Emmet-Teller (BET) method and Barrett-Joyner-Halenda (BJH) method, respectively, wherein the BET method is based on the Multilayer molecular adsorption theory and the BJH method is based on a developed Kelvin capillary condensation theory.[30]

Field emission scanning electron microscopy (FE-SEM) was performed on a Hitachi S4800 Field Emission Scanning Electron Microscopy.

High-resolution transmission electron microscopy (HRTEM) images were recorded on a JEM-2010 EX microscope equipped with X-Ray microanalyzer EDX, which was operated at an accelerating voltage of 200 kV. The samples were crushed in A.R. grade ethanol and

RSC Advances Accepted Manuscript

the resulting suspension was allowed to dry on carbon film supported on copper grids.

The catalytic reduction of 4-nitrophenol was detected by UV-visible absorption spectra and its results were recorded using a BLV-GHX-V ultraviolet spectrophotometer.

The silver contents were analyzed using Jarrell-Ash 1100 Inductively Coupling Plasma spectrometer (ICP). Before analysis, the silver NPs in the sample were dissolved by adding nitric acid, and then the hydrofluoric acid was added to dissolve the mesoporous silica.

2.4. Catalytic test

The catalytic performance of the Ag@meso-SiO_2 was evaluated using the liquid-phase reduction of 4-nitrophenol (4-NP) to 4-aminophenol (4-AP) with a $NaBH_4$ aqueous solution at room temperature. The catalytic reaction was carried out in a quartz cuvette and monitored by in situ measuring the UV-vis absorption spectra. Typically, 0.1 mL of the aqueous solution of 4-NP (0.005 M), 1 mL of deionized water and 1 mL of aqueous solution of fresh $NaBH_4$ (0.15 M) were added into a quartz cuvette, followed by addition of 0.5 mL of Ag@meso-SiO_2 nanocatalyst (0.2, 0.3 and 0.5 mg/mL in aqueous solution) respectively. In addition, the different systems for this reduction reaction based on the pure mesoporous silica, commercial Ag NPs, Ag/SBA-15 and single core Ag@SiO_2 were investigated under the same conditions. The gradual change of the solution color from light bright yellow to colorless was observed during the reaction. Finally, the recycling tests were conducted to evaluate the stability of catalysts.

3. Results and Discussion

Scheme 1 illustrates the synthetic procedure of the multiple-Ag-cores hollow

RSC Advances Accepted Manuscript

mesoporous silica sphere Ag@meso-SiO_2. The synthesized method is based on a modified sacrificed template route involving the Ag-aminosilane modification of carbon sphere, cladding of mesoporous silica, and removing of template. Firstly, carbon nanosphere is prepared via the hydrothermal method of glucose. In the next step, the aminosilane of APTES is tethered on carbon nanosphere by reacting with the hydroxyl of carbon sphere surface to endow the surface of carbon sphere with abundant ligands. The presence of amino groups on the carbon sphere could efficiently anchor metal ions. Subsequently, Ag ions are anchored on the surface of aminosilane modified carbon spheres via coordinated interaction with -NH_2 of APTES. After that, siliceous oligomers attaching cationic micelles coat on the functionalized carbon sphere to obtain the initial microreactor. Finally, the organic species of micelles and carbon sphere are removed by the heat treatment, and the multiple Ag NPs, hollow cavity and mesoporous shell are in situ produced during the hollowing process.

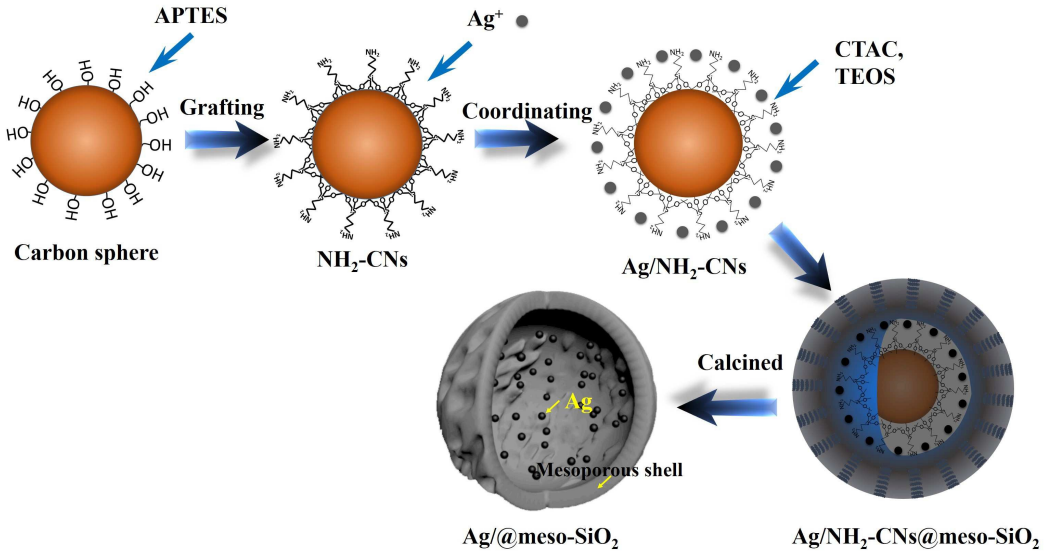

Scheme 1 The synthetic illustration for the preparation of Ag@meso-SiO_2

RSC Advances Accepted Manuscript

Wide-angle XRD results

The wide-angle XRD patterns of all the samples are presented in Fig. 1. All samples exhibit a broad diffraction peak from 20° to 30°. The broad peak presenting on the curves of samples CNs and Ag/NH_2-CNs are ascribed to amorphous carbon. While the broad peaks of other two samples are in accordance with that of amorphous silica. Additionally, it is worth noting that there are no other peaks detected in the curves of sample Ag/NH_2-CNs and as-synthesized Ag/NH_2-CNs@SiO_2, suggesting no formation of the crystalline Ag NPs before the hollowing process. With regard to the calcined Ag@meso-SiO_2, several newly emerging crystal diffraction peaks at 38°, 44°, 64° and 77° are observed and indexed to the (111), (200), (220) and (311) crystal diffraction for Ag nanocrystals. The result demonstrates the formation of Ag cores within the silica shell during the thermal process. In addition, on the basis of the Scherrer's Equation, the calculated average size of generated Ag NPs is 17.4 nm.

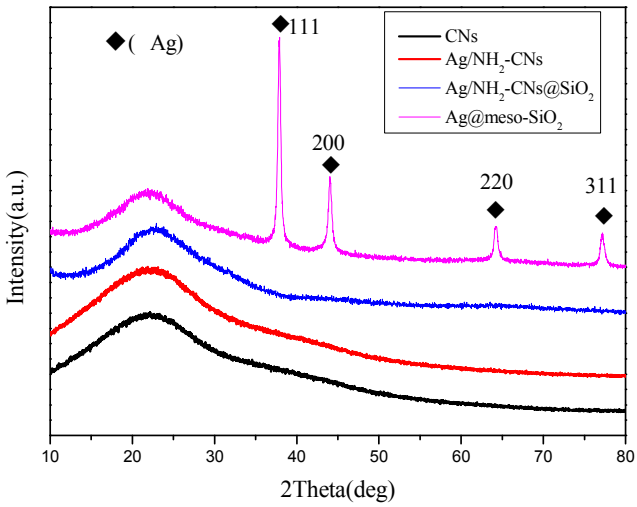

Fig. 1 Wide-angle XRD patterns of CNs, Ag/NH_2-CNs, Ag/NH_2-CNs@SiO_2 and Ag@meso-SiO_2

RSC Advances Accepted Manuscript

FT-IR results

FT-IR spectra were employed for testing groups' information of different modified samples and their results are exhibited in Fig. 2. As shown above, as compared with bare carbon nanosphere, aminosilane-modified carbon sphere shows a set of additional peaks at 1090 and 460 cm^{-1} which ascribed to the asymmetric stretching vibrations and bending vibrations of Si-O.[31] These new feature absorbed peaks confirm the presence of aminosilane and the successful grafting of APTES on the surface of carbon sphere. With regard to the sample of Ag/NH_2-CNs@SiO_2, the absorbed peaks ascribed to Si-O obviously became stronger as compared with the carbon sphere modified with APTES. This phenomenon supports the deposition and coating of siliceous species on the carbon sphere. Finally, with the heat treatment, it is evident that the absorbed bands of APTES, micelle template and carbon sphere obviously disappear, the remaining peaks are coincided with feature absorption of the typical mesoporous silica, which indicates the organic species and carbon sphere are mostly removed.

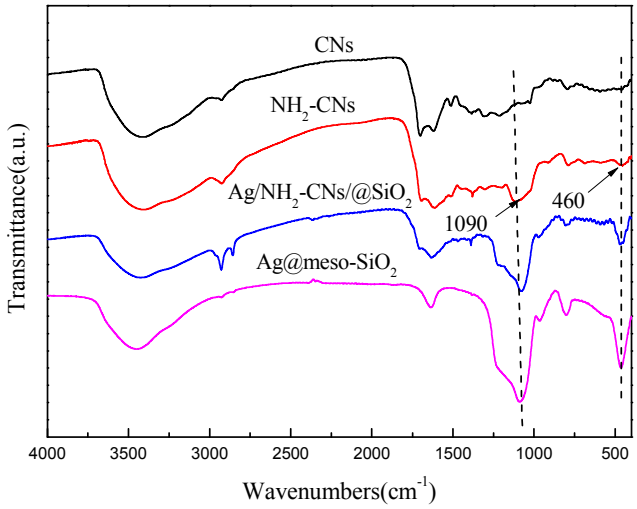

RSC Advances Accepted Manuscript

Fig. 2 FT-IR spectra of corresponding samples of CNs, NH_2-CNs, Ag/NH_2-CNs@SiO_2 and Ag@meso-SiO_2.

XPS results

In order to demonstrate the chemical environment of elements, the XPS spectra are utilized to test the samples of NH_2-CNs and Ag/NH_2-CNs. As shown above, Fig. 3 shows the representative survey of XPS spectrum of N 1s. Wherein, the N 1s spectrum (Fig. 3a) for NH_2-CNs show two clear peaks of binding energy at about 399.75 and 401.65 eV, which are attributed to the free amine groups and protonated amine groups of APTES, respectively.[32] The presence of protonated amine group is due to the protonation of aminopropyl groups of APTES in the presence of H^+. Whereas, the N 1s spectrum (Fig. 3b) for Ag/NH_2-CNs obviously gives three characteristic peaks of binding energy located at 406.91 eV, 401.47eV and 399.75 eV. The presence of feature peak at 399.75 eV should be attributed to free amino groups. It is noticeable that another feature peak at 401.47 eV apparently differs from its counterpart in the N1s spectrum of NH_2-CNs with an obvious shift to low binding energy. Meanwhile, the enhanced intensity of this characteristic peak is observed as compared to the peak of free amino group. This result indicates that the presence of this feature peak should be associated with coordination of Ag ions on the amino group of APTES. Furthermore, based on this result, the amino groups coordinated with Ag^+ are dominated in the surface of modified carbon sphere. Finally, it should be noted that an additional peak at 406.91 eV is observed, according to the ref.,[32] the presence of the feature peak should be ascribed to nitrate ion matched with Ag ions presenting on the

RSC Advances Accepted Manuscript

surface of functional carbon sphere. Taken together, these results strongly support the coordination of Ag ions on the aminosilane modified carbon sphere.

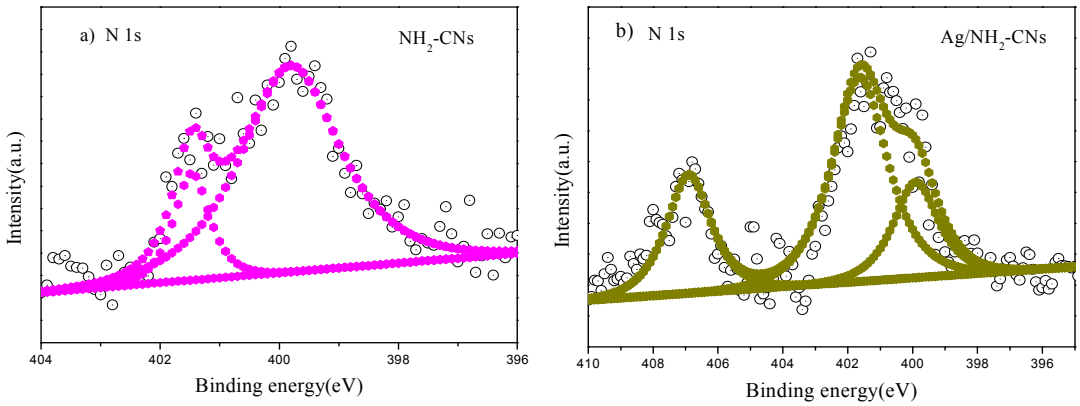

Fig. 3 XPS N 1s spectra of NH_2-CNs (a) and silver-loaded Ag/NH_2-CNs (b).

Low-angle XRD results

The low-angle XRD pattern of Ag@meso-SiO_2 is displayed in Fig. 4. A diffraction peak at 2θ=2-3° can be observed which is ascribed to the typical 100 peak of mesophase. The presence of this characteristic peak indicates a mesostructure of the material.

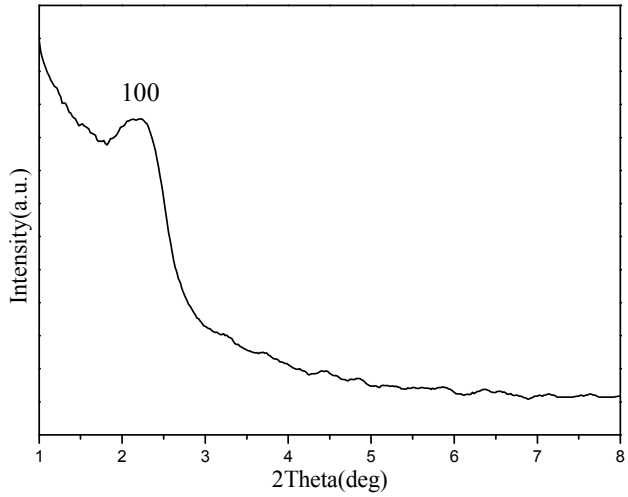

Fig. 4 Low-angle pattern of the sample of Ag@meso-SiO_2

RSC Advances Accepted Manuscript

N_2-adsorption/desorption results

The structural properties of the sample of Ag@meso-SiO_2 hollow sphere are further investigated using N_2-adsorption/desorption analysis and its result is shown in Fig. 5. The isotherm exhibits the type IV curves with H1 hysteresis loop, which are typical characteristics of mesoporous materials. This result suggests that the sample of Ag@meso-SiO_2 preserves mesoporous structure after removing template of carbon sphere and surfactants. Additionally, the surface area and total pore volume are calculated to be as large as 622 m^2/g and 0.59 cm^3/g, respectively. Additionally, according to the BJH model, the Ag@meso-SiO_2 hollow nanospheres have a pore size distribution of approximately 3.29 nm (Fig. 5b, inset). This result reveals that the functional microreactor possesses large surface area and pore volume which would provide broad diffused passageway for the chemicals transported in and out.

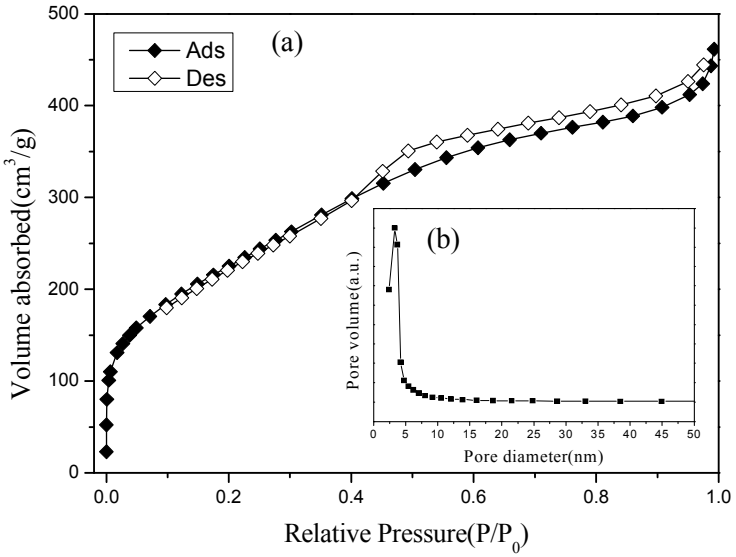

Fig. 5 N_2 adsorption/desorption isotherms (a) and pore size distribution (b, inset) of Ag@meso-SiO_2

RSC Advances Accepted Manuscript

SEM results

The representative SEM images of the samples of Ag/NH_2-CNs, as-synthesized Ag/NH_2-CNs@SiO_2 and Ag@meso-SiO_2 are displayed in Fig. 6. As shown above, the Fig. 6a gives the image for sample of Ag/NH_2-CNs, indeed, the obvious spherical morphology can be observed even with modification of Ag ions and aminosilane. Meanwhile, associating with EDX result of sample of Ag/NH_2-CNs, the signal peaks of element of C, O, Si and Ag can be obviously detected. The presence of element of Si and Ag in the EDX pattern strongly demonstrates the successful grafting of APTES and anchoring of Ag ions. Additionally, no aggregated Ag nanoparticles are detected on the surface of Ag/NH_2-CNs, which indicates that Ag species should be existed with the form of ions on the surface of carbon sphere. When the sample of Ag/NH_2-CNs is coated by mesoporous siliceous species, the spherical morphology has not been changed. After calcining under the air, the round-like morphology for the sample of Ag@meso-SiO_2 is exhibited in the Fig. 6c, and the size of the core-shell Ag@meso-SiO_2 is about 400 nm. Additionally, an obvious hollow status of sphere can be observed in the every image (wherein, an obvious broken sphere is marked with yellow circle). It is noteworthy that the corrugate and shrinking silicate shell presents in the hollow spheres. The surface of Ag@meso-SiO_2 in a wrinkle state should be due to the shrink of silicate shell during the annealed process. However, the resulting product with hollow cavity do not present collapsed or fractured status. This phenomenon strongly demonstrates the good structural integrity of hollow and multi-core sphere. Meanwhile, it is observed that the synthesized mesoporous spheres also possess a well-dispersed state without obvious aggregation and crosslinking.

RSC Advances Accepted Manuscript

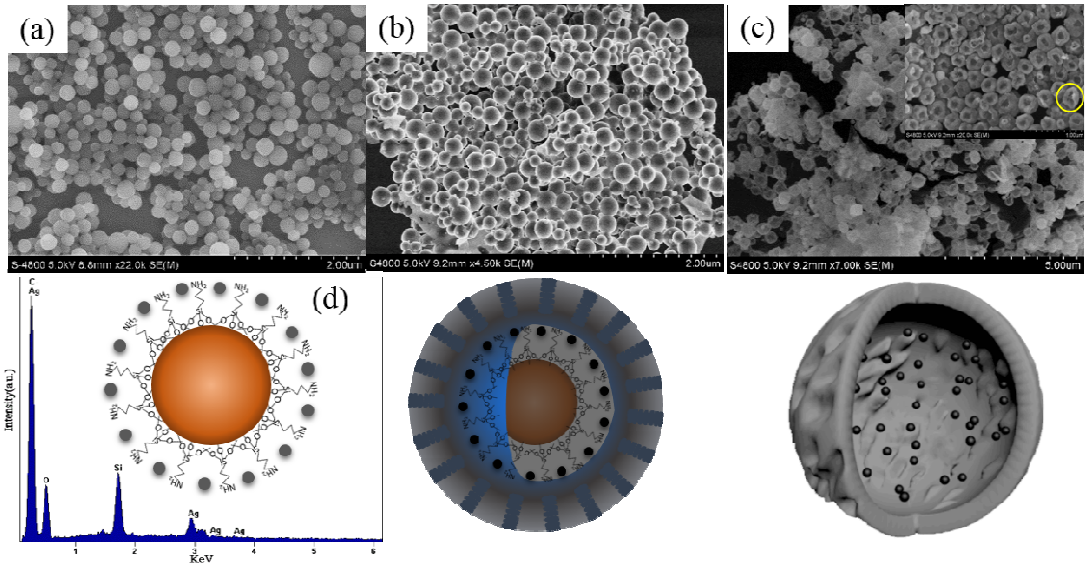

Fig. 6 Representative SEM images of samples of Ag/NH_2-CNs (a), Ag/NH_2-CNs@SiO_2 (b) and Ag@meso-SiO_2 (c) and EDX pattern (d) of sample Ag/NH_2-CNs.

TEM results

The morphologies and structure of the prepared Ag@meso-SiO_2 nanospheres and status of Ag nanoparticles were characterized by transmission electron microscopy (TEM) and their result are shown in Fig. 7. The cores@shell structure can be demonstrated in TEM images. The representative TEM images of Ag@meso-SiO_2 (Fig. 7a and b) reveal that the as-prepared Ag@meso-SiO_2 particles possess well-defined core-shell structures with multiple free Ag cores nicely encapsulated in hollow mesoporous shells. Additionally, the free Ag cores are well separated in the hollow cavity. It is well-documented that several-in-one encapsulation of noble metal nanoparticles in hollow shells can effectively prevent the aggregation of active nanoparticles and therefore significantly improve their catalytic stability. Besides, the shell of Ag@meso-SiO_2 with thickness of ca. 50 nm exhibits slightly corrugated façade. The phenomenon should be associated with shrink of silicate

RSC Advances Accepted Manuscript

shell during heat treatment. However, it is worth noting that no massive collapsed hollow mesoporous spheres are detected in the TEM images, which indicates that the shrink during the heat treatment do not result in the deterioration of the whole structure. By comparing the TEM (Fig. 7) and XRD (Fig. 1) results, it can be found that these results favor the formation of small Ag particles. And the average size calculated from the TEM result is 17.6 nm, which is in agreement with the calculated result from wide-angle XRD.

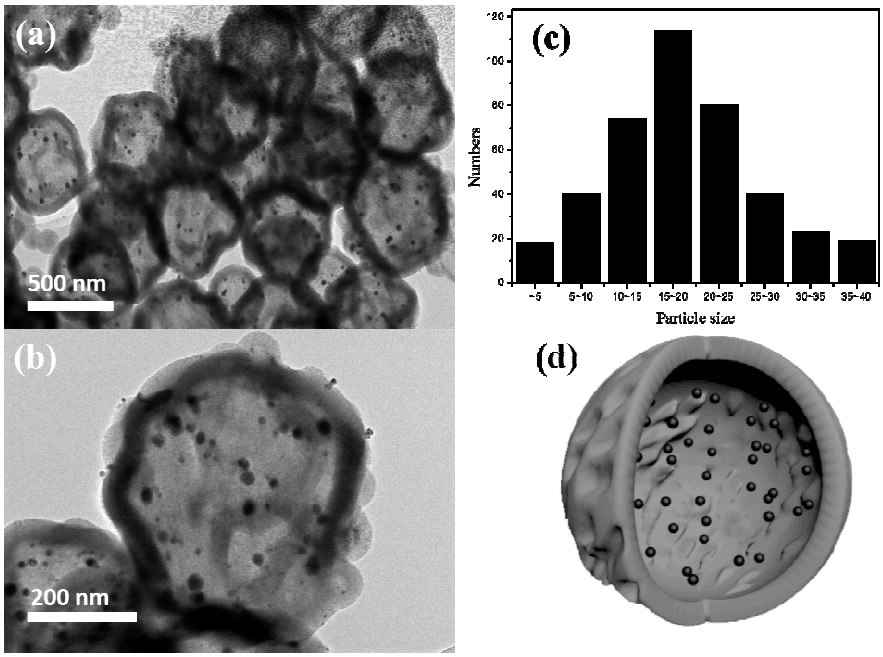

Fig. 7 Representative TEM images of Ag@meso-SiO_2 (a) and (b), particle size distribution of Ag in the image of a (c) and image of designed targeted product

Catalytic analysis

The catalytic performance of the Ag@meso-SiO_2 hollow microreactor was investigated by using the liquid-phase reduction of 4-NP by $NaBH_4$ to 4-AP (Fig. 8a). Adding of $NaBH_4$ into the aqueous solution of 4-NP will lead to the color change of solution from light yellow to light bright yellow. Moreover, the UV-vis absorption peak shifting from 317 to

RSC Advances Accepted Manuscript

400 nm can be observed in Fig. 8a because of the deprotonation of 4-NP and the formation of 4-AP. No obvious change of the UV-vis absorption spectra was measured after 24 h, suggesting that the reduction reaction did not start without the Ag@meso-SiO_2 hollow nanosphere catalysts (not given). Additionally, a similar result is also observed for the system just using pure mesoporous silica as catalyst (Table 1), which indicates that Ag NPs act as the catalytic active centers of the reduction of 4-NP. While, the mesoporous shell just provides a protective environment for this reaction. After the addition of Ag@meso-SiO_2, the reduction reaction started immediately, and the color of the reaction solution turned lighter and lighter. The absorption intensity at 400 nm became weaker and weaker along with the increase of reaction time, at the same time, an absorption peak around 317 nm appeared due to the formation of 4-AP (Fig. 8a).

Due to the number influence of catalytic active centers for reaction activity in catalytic process, enough active site numbers would extremely promote the reaction rates of reduction reaction. This is due to the presence of increasing unsaturated catalytic active adsorbed sites in reaction. Therefore, herein, the affecting of catalyst amount of Ag@meso-SiO_2 on the reduction reaction was investigated. The C/C_0 versus reaction time for the reduction of 4-NP using different amounts of Ag@meso-SiO_2 as catalysts are displayed in Fig. 8b, where C and C_0 are the concentration of 4-NP at different times and initial time, which can be measured from the relative intensity of the absorbance C and C_0, respectively. As shown in Fig. 8b, the biggest using amount of Ag@meso-SiO_2 obviously shows the fastest reaction rate in the reduction process. Additionally, the linear relationship using different amounts of catalyst between $\ln(C/C_0)$ and reaction time of the reduction

RSC Advances Accepted Manuscript

reaction is demonstrated in Fig. 8c. It is obvious that using higher amount of catalyst leads to a quicker reaction rate in the reaction process. This result suggests that the concentration of Ag@meso-SiO_2 have certain effects on the catalytic reaction rate. However, at the time of initial reaction, the reaction is dominated by the diffused process, therefore, the linear relationship of initial point does not well locate in the fitting line between $\ln(C/C_0)$ and reaction time, similarly, a result could be observed in the reported literature.[33] We suggest that the reactants may firstly diffuse across mesopores of the silica shells and subsequently interact with the Ag cores with catalytic activity. Herein, the liquid-phase reduction reaction can be assumed to follow pseudo-first-order expression[34]: $\ln(C_0/C)=kt$, where C_0/C is the normalized organic compounds concentration and k is the apparent reaction rate (min^{-1}). By plotting $\ln(C/C_0)$ as a function of reduction time through linear regression started from the second point, the k constant can be obtained from the slopes of the simulated straight lines. The k constant from the calculation corresponding to different amounts of catalyst from 0.2 mg/L, 0.3 mg/L and 0.5 mg/L are 0.399, 0.727 and 0.829 min^{-1}. Judging from the calculated result of reaction rate constant, the reduction reaction rate of 4-NP is obviously influenced by the using amounts of Ag@meso-SiO_2. The catalytic reaction rate of 4-NP reduction is reached to the maximum when the using amount of Ag@meso-SiO_2 is largest. However, it should be noted that the increasing catalyst amounts do not lead to the linear increase of the reaction rate. The influence of catalyst concentration on the reaction rate has tended to be saturated when using 0.3 mg/mL of Ag@meso-SiO_2. Therefore, an added catalyst concentration of 0.4 mg/mL was applied in this reaction and its reaction rate was calculated. For a quantitative comparison, the activity

RSC Advances Accepted Manuscript

parameter k_{app} = k/M(mass) was introduced and defined as the ratio of the rate constant k to the weight of the catalyst added.[34, 35] By comparison, it is discovered that the excessive catalysts lead to the decreasing of the normalized k_{app} of Ag@meso-SiO_2 even with a close reaction rate for the different catalyst concentrations of 0.4 and 0.5 mg/mL. This may be attributed to the presence of unsaturated adsorbed sites on the Ag cores due to the excess of catalyst.

In addition, in order to investigate the specificity of Ag@meso-SiO_2 system, several different catalytic systems using commercial Ag NPs, Ag-supported SBA-15 and single core Ag@SiO_2 are compared. Obviously, the Ag-supported SBA-15 exhibits the highest catalytic reaction rate as compared with commercial Ag NPs, Ag@meso-SiO_2 and single core Ag@SiO_2. This result is attributed to the largest expose of Ag active particle on the surface of mesoporous silica, therefore, the contact of reactant molecule with Ag is more accessible. While, as compared to the single core Ag@SiO_2, the Ag@meso-SiO_2 obviously exhibits the bigger superiority in catalytic reaction rate. This should be assignable to the presence of multiple Ag cores, which extremely increases the contact chance between reactant molecules and Ag cores. In addition, the recycling experiments for the reduction of 4-NP using Ag@meso-SiO_2, Ag/SBA-15 and single core Ag@SiO_2 are conducted and their results are displayed in Fig. 8d. Just as observed in this figure, even with six employments in reduction reaction, no obvious dropping in catalytic activity is observed for the Ag@meso-SiO_2. However, it is noteworthy that the Ag/SBA-15 shows a dropped trend in catalytic activity. This is due to the missing of Ag species in reaction process without the protection of mesoporous shell.

RSC Advances Accepted Manuscript

Table 1 Comparison of the reaction parameters with different catalyst systems

Samples	Ag/Si (%)	Dose (mg/mL)	Reaction Time (min)	k/min^{-1}	Normalized k_{app}(min^{-1}/mg)
Meso-SiO_2	0	0.3	8	0	0
Ag@meso-SiO_2	1.56	0.2	8	0.399	3.99
	1.56	0.3	5	0.727	4.84
	1.56	0.4	4	0.825	4.13
	1.56	0.5	4	0.829	3.32
Ag NPs	-	0.3	15	0.167	1.11
Ag/SBA-15	1.49	0.3	4	0.865	5.76
Ag@SiO_2	3.5	0.3	10	0.306	2.04

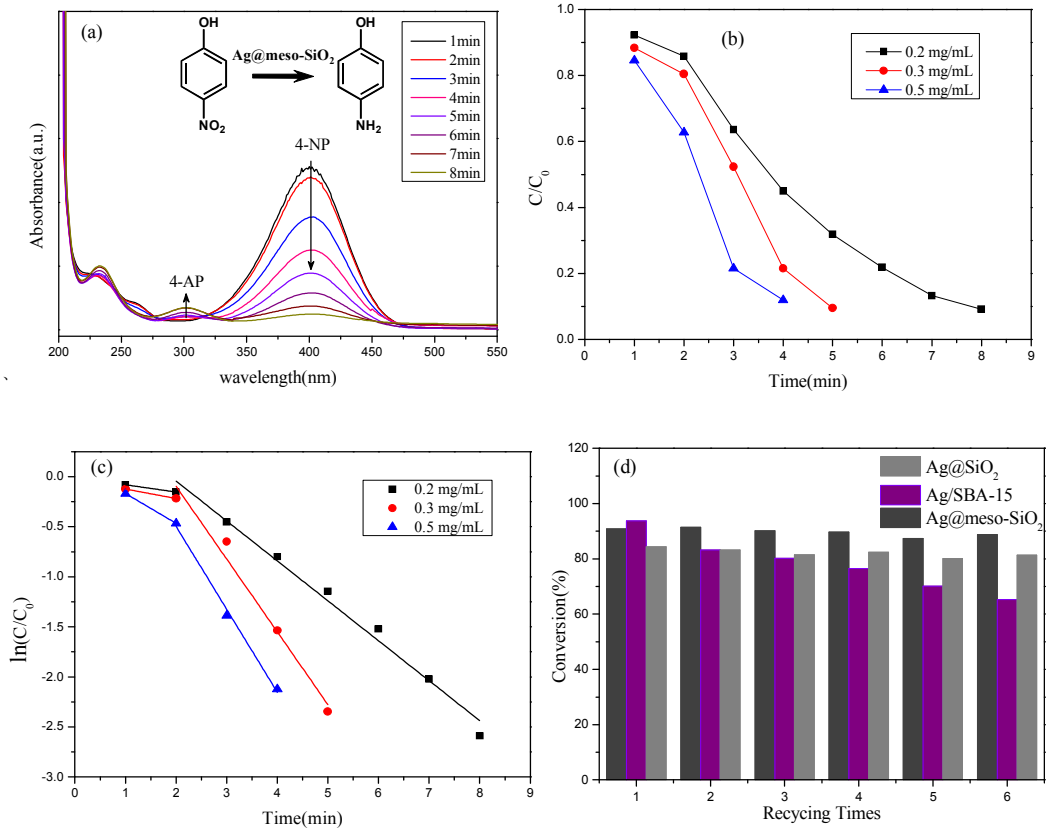

Fig. 8 Time-dependent UV-vis spectral changes of the reaction mixture catalyzed using 0.2

RSC Advances Accepted Manuscript

mg/L of Ag@meso-SiO_2 microreactor (a). C/C_0 versus reaction time for the reduction of 4-NP using different amounts of Ag@meso-SiO_2 as catalysts (b). Plot of $\ln(C/C_0)$ versus reduction time for the reduction of 4-NP using different amounts of Ag@meso-SiO_2 catalyst (c). Recycling test results for different catalysts of single core Ag@SiO_2, Ag/SBA-15 and Ag@meso-SiO_2 (d).

4. Conclusions

In summary, we successfully fabricated a noble metal functionalized catalyst with desired dispersed Ag cores, hollow cavity and mesoporous shell structures using a new constructed approach, which is regarded as an ideal candidate for microreactor just like Cores@Shell architecture. The strategy offered the possibility for confining noble metal NPs in host material by a novel idea. The as-prepared Ag@meso-SiO_2 has been successfully used as reduced catalyst and exhibited high catalytic performances in the liquid-phase reduction of 4-NP and the increasing dosage of catalyst facilitate to enhance the catalytic performance. The present method is versatile, and potentially many noble metals, transition metals and their bimetallic nanoparticles can be resided inside the hollow mesoporous silica sphere via this process.

Acknowledgements

The authors acknowledge the project Funded by the Priority Academic Program Development of Jiangsu Higher Education Institutions (PAPD) and the financial support of the National Natural Science Foundations of China (21276125, 20876077 and 21476108).

RSC Advances Accepted Manuscript

Notes and References

1 Y. F. Zhu, J. L. Shi, W. H. Shen, X. P. Dong, J. W. Feng, M. L. Ruan and Y. S. Li, *Angew. Chem. Int. Edit.*, **2005**, 44, 5083-5087.

2 F. Tang, L. Li and D. Chen, *Adv. Mater.*, **2012**, 24, 1504-1534.

3 W. J. Li, X. X. Sha, W. J. Dong and Z. C. Wang, *Chem. Commun.*, **2002**, 2434-2435.

4 F.-P. Chang, Y.-P. Chen and C.-Y. Mou, *Small*, **2014**, 10, 4785-4795.

5 L. Zhou, Z. Chen, K. Dong, M. Yin, J. Ren and X. Qu, *Adv. Mater.*, **2014**, 26, 2424-2430.

6 Y. Zhao, L.-N. Lin, Y. Lu, S.-F. Chen, L. Dong and S.-H. Yu, *Adv. Mater.*, **2010**, 22, 5255-5259.

7 X. Fang, X. Zhao, W. Fang, C. Chen and N. Zheng, *Nanoscale*, **2013**, 5, 2205-2218.

8 Y. Li and J. Shi, *Adv. Mater.*, **2014**, 26, 3176-3205.

9 J. Liu, H. Q. Yang, F. Kleitz, Z. G. Chen, T. Yang, E. Strounina, G. Q. Lu and S. Z. Qiao, *Adv. Funct. Mater.*, **2012**, 22, 591-599.

10 X. Fang, Z. Liu, M.-F. Hsieh, M. Chen, P. Liu, C. Chen and N. Zheng, *Acs Nano*, **2012**, 6, 4434-4444.

11 S. M. Kim, M. Jeon, K. W. Kim, J. Park and I. S. Lee, *J. Am. Chem. Soc.*, **2013**, 135, 15714-15717.

12 J. Lee, J. C. Park and H. Song, *Adv. Mater.*, **2008**, 20, 1523-1538.

13 C. Liu, J. Li, J. Qi, J. Wang, R. Luo, J. Shen, X. Sun, W. Han and L. Wang, *Acs Appl. Mater. Interf.*, **2014**, 6, 13167-13173.

14 Q. Yang, D. Han, H. Yang and C. Li, *Chem. Asian J.*, **2008**, 3, 1214-1229.

15 Z. Chen, Z.-M. Cui, F. Niu, L. Jiang and W.-G. Song, *Chem. Commun.*, **2010**, 46, 6524-6526.

16 M. Xiao, C. Zhao, H. Chen, B. Yang and J. Wang, *Adv. Funct. Mater.*, **2012**, 22, 4526-4532.

17 H. Wang, J.-G. Wang, H.-J. Zhou, Y.-P. Liu, P.-C. Sun and T.-H. Chen, *Chem. Commun.*, **2011**, 47, 7680-7682.

18 Y. Chen, Q. Wang and T. Wang, *Dalton Trans.*, **2015**, 44, 8867-8875.

19 C. Liu, J. Li, J. Wang, J. Qi, W. Fan, J. Shen, X. Sun, W. Han and L. Wang, *Rsc Adv.*, **2015**, 5, 17372-17378.

20 Y. Yang, W. Zhang, Y. Zhang, A. Zheng, H. Sun, X. Li, S. Liu, P. Zhang and X. Zhang, *Nano Res.*, **2015**, 8, 3404-3411.

21 S. H. Liu and M. Y. Han, *Adv. Funct. Mater.*, **2005**, 15, 961-967.

22 S. Liu, Y. Wong, Y. Wang, D. Wang and M.-Y. Han, *Adv. Funct. Mater.*, **2007**, 17, 3147-3152.

23 J. Pak and H. Yoo, *Micropor. Mesopor. Mater.*, **2014**, 185, 107-112.

24 J. Chen, Z. Xue, S. Feng, B. Tu and D. Zhao, *J. Colloid Interf. Sci.*, **2014**, 429, 62-67.

25 Y. Zhang, S. Xiang, Y. Zhou, Y. Xu, Z. Zhang, X. Sheng, Q. Wang and C. Zhang, *Rsc Adv.*, **2015**, 5, 48187-48193.

26 Y. Chen, Q. Wang and T. Wang, *Dalton Trans.*, **2013**, 42, 13940-13947.

27 F. Wei, C. Cao, Y. Sun, S. Yang, P. Huang and W. Song, *Chemcatchem*, **2015**, 7, 2475-2479.

28 W. P. Zhu, Y. C. Han and L. J. An, *Micropor. Mesopor. Mater.*, **2005**, 80, 221-226.

29 P. Saint-Cricq, J. Wang, A. Sugawara-Narutaki, A. Shimojima and T. Okubo, *J. Mater. Chem. B*, **2013**, 1, 2451-2454.

30 M. Kruk, M. Jaroniec and A. Sayari, *Langmuir*, **1997**, 13, 6267-6273.

31 Y. Kong, H. Y. Zhu, G. Yang, X. F. Guo, W. H. Hou, Q. J. Yan, M. Gu and C. Hu, *Adv. Funct. Mater.*, **2004**, 14, 816-820.

32 H. Yu, Y. Zhu, H. Yang, K. Nakanishi, K. Kanamori and X. Guo, *Dalton Trans.*, **2014**, 43, 12648-12656.

RSC Advances Accepted Manuscript

33 J. Gao, J. Xu, S. Wen, J. Hu and H. Liu, *Micropor. Mesopor. Mater.*, **2015**, 207, 149-155.
34 Z. Dong, X. Le, X. Li, W. Zhang, C. Dong and J. Ma, *Appl. Catal. B-Environ.*, **2014**, 158, 129-135.
35 B. Baruah, G. J. Gabriel, M. J. Akbashev and M. E. Booher, *Langmuir*, **2013**, 29, 4225-4234.

RSC Advances Accepted Manuscript

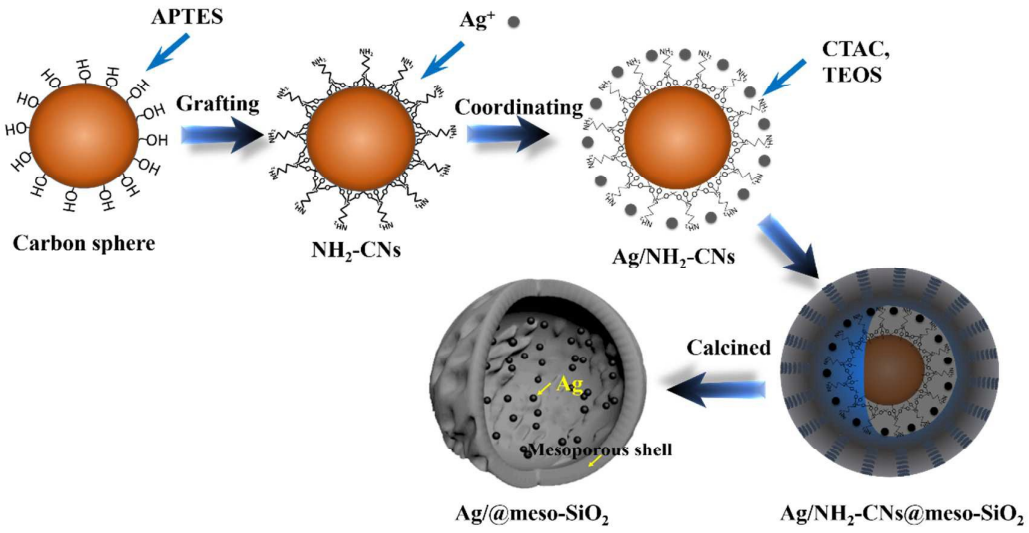

Scheme 1 The synthetic illustration for the preparation of Ag@meso-SiO_2

In this paper, a Cores@Shell structure of microreactor with well-dispersed active phase of multiple movable Ag-cores, hollow cavity and protective mesoporous shell was prepared by a simple and novel constructed approach. The organic ligand of aminosilane (APTES) was directly incorporated on the carbon nanosphere to anchor Ag ions as metallotemplate, which avoids conventional methods of tedious steps, and then the sacrificed metallotemplate was employed for directly fabricating the special hollow mesoporous silica microreactor. As a result, multiple movable active Ag-cores were in situ produced and encapsulated in cavity of hollow mesoporous silica during the thermal process. Mobility of the active Ag-cores extremely improved the catalytic performance by enhancing their collision frequency with reactant molecules. Just as expected, the catalyst as a functional microreactor exhibited a high catalytic activity for the liquid-reduction of 4-nitrophenol and the increasing dosage of used catalyst contributes to the enhancing of catalytic activity. The methodology demonstrated here provides a new insight for the fabrication of versatile functional nanosmaterials with kinds of noble or transition metals inside hollow shell.

RSC Advances Accepted Manuscript